ARTICLES

Lattice and spin polarons in two dimensions

Y. Zhao and G. H. Chen
Department of Chemistry, University of Hong Kong, Hong Kong, China

L. Yu
Abdus Salam International Centre for Theoretical Physics, P.O. Box 586, 34100 Trieste, Italy and Institute of Theoretical Physics, Academia Sinica, P.O. Box 2735, Beijing 100080, China

(Received 22 March 2000; accepted 25 July 2000)

A variational approach is employed to compute the wave function of a single polaron for a two-dimensional Holstein Hamiltonian with arbitrary forms of linear particle–boson interactions and boson dispersion relations. The Toyozawa ansatz is utilized, and generalizations to multiple polarons are outlined. Applications are made to model superradiance in pseudoisocyanine bromide *J*-aggregates, and to calculate quasiparticle dispersion of an itinerant hole in a two-dimensional antiferromagnet. © *2000 American Institute of Physics.* [S0021-9606(00)50240-2]

I. INTRODUCTION

Over the last fifty years the problem of a few fermions interacting with a bath of bosons has attracted enduring interest which encompasses many branches of physics and chemistry. Systems of electrons and phonons, for example, are found to constitute some of the simplest yet rich structures in condensed phase. The interest sometimes extends beyond physical descriptions of materials. The field has been a testing ground for various theoretical techniques, including the first application of field theories to condensed matter physics. Recent applications of the theories are found in the context of low dimensional systems such as CuO_2-based materials,[1] quantum wires,[2] superfluids,[3] and molecular aggregates.[4–9]

In this article we are concerned with a two-dimensional Holstein Hamiltonian and its applications to superradiance in peudoisocyanine bromide (PIC-Br) *J*-aggregates and quasiparticle dispersion in hole-doped antiferromagnets. The purpose here is two-fold. First, we would like to establish a general method to treat two-dimensional systems of a few fermions coupled to a bath of bosons. The method needs to be general enough to accommodate various forms of fermion–boson interactions, and at the same time, efficient enough to offer practical solutions with adequate precision. Second, we seek to offer insights to real systems which are described by the two-dimensional fermion-bath (or exciton-bath) model. We take, as two examples, the PIC-Br *J*-aggregates and the hole-doped antiferromagnets. The former is recently argued by Potma and Wiersma[6] to be a two-dimensional exciton–phonon system exhibiting the superradiance behavior.[4] The latter is a hole–magnon system on a square lattice whose resemblance to the lattice polaron is a matter of much current interest.[10–15]

The article is organized as follows. In Sec. II we describe the Hamiltonian and methodology. In the following two sections we apply our approach to two problems of contemporary interest, namely, superradiance in PIC-Br *J*-aggregates of a brick-work structure, and hole motion in antiferromagnets of insulating cuprate $Sr_2CuO_2Cl_2$. Discussions are presented in Sec. V.

II. FORMULATION

The Holstein Hamiltonian with off-diagonal particle–boson interactions included reads

$$\hat{H}=\sum_{\mathbf{k}} J_{\mathbf{k}} a_{\mathbf{k}}^{\dagger} a_{\mathbf{k}}+\sum_{\mathbf{q}} \omega_{\mathbf{q}} b_{\mathbf{q}}^{\dagger} b_{\mathbf{q}} + \frac{1}{\sqrt{N}} \sum_{\mathbf{kq}} (M_{\mathbf{k},\mathbf{q}} a_{\mathbf{k}-\mathbf{q}}^{\dagger} a_{\mathbf{k}} b_{\mathbf{q}}^{\dagger}+\text{H.c.}), \tag{2.1}$$

where $a_{\mathbf{k}}^{\dagger}(a_{\mathbf{k}})$ creates (annihilates) a particle (exciton or hole) of momentum $\mathbf{k}$, $b_{\mathbf{q}}^{\dagger}(b_{\mathbf{q}})$ creates (annihilates) a boson (phonon or magnon) of momentum $\mathbf{q}$. $J_{\mathbf{k}}$ is the bare particle band, $\omega_{\mathbf{q}}$ is the boson dispersion relation, $M_{\mathbf{k},\mathbf{q}}$ is the particle–boson coupling, and H.c. is short for Hermitian conjugate. N is the number of sites.

The one-dimensional Holstein Hamiltonian with diagonal and off-diagonal coupling to Einstein phonons was successfully modeled by a variational wave function pioneered by Toyozawa (the Toyozawa ansatz) and its generalizations.[16–18] The variational methods are shown to be rather efficient while remaining quantitatively accurate compared with calculations involving far more expensive computational resources.[19,20] The Toyozawa ansatz for the Hamiltonian (2.1) utilizes boson coherent states:

$$|\Phi^{\mathbf{K}}\rangle = N^{-1}\sum_{\mathbf{nk}} e^{i(\mathbf{K}-\mathbf{k})\cdot\mathbf{n}}\psi_{\mathbf{k}}^{\mathbf{K}}a_{\mathbf{k}}^{\dagger} \times \exp\left[-N^{-1/2}\sum_{\mathbf{q}}(\lambda_{\mathbf{q}}^{\mathbf{K}}e^{-i\mathbf{q}\cdot\mathbf{n}}b_{\mathbf{q}}^{\dagger}-\lambda_{\mathbf{q}}^{\mathbf{K}*}e^{i\mathbf{q}\cdot\mathbf{n}}b_{\mathbf{q}})\right]|0\rangle. \tag{2.2}$$

Here $\mathbf{K}$ is the crystal momentum, $\psi_{\mathbf{k}}^{\mathbf{K}}$ and $\lambda_{\mathbf{q}}^{\mathbf{K}}$ are the variational parameters characterizing the boson distortion and the particle amplitude, respectively. $|0\rangle$ is vacuum for both the particle and the boson excitation. The Toyozawa ansatz (2.2) neglects explicit instantaneous correlations between the particle and the boson. We note that the wave function (2.2) is in general not normalized. The variational energy $E_{\mathbf{K}}$ is given by the expectation value of $\hat{H}$,

$$E_{\mathbf{K}} \equiv \frac{H^{\mathbf{K}}}{N^{\mathbf{K}}}, \tag{2.3}$$

where

$$H^{\mathbf{K}} = \langle\Phi^{\mathbf{K}}|\hat{H}|\Phi^{\mathbf{K}}\rangle, \tag{2.4}$$

$$N^{\mathbf{K}} = \langle\Phi^{\mathbf{K}}|\Phi^{\mathbf{K}}\rangle. \tag{2.5}$$

Minimization of $E_{\mathbf{K}}$ requires

$$\frac{\partial H^{\mathbf{K}}}{\partial\lambda_{\mathbf{q}}^{\mathbf{K}*}} - \frac{H^{\mathbf{K}}}{N^{\mathbf{K}}}\frac{\partial N^{\mathbf{K}}}{\partial\lambda_{\mathbf{q}}^{\mathbf{K}*}} = 0, \tag{2.6}$$

$$\frac{\partial H^{\mathbf{K}}}{\partial\psi_{\mathbf{q}}^{\mathbf{K}*}} - \frac{H^{\mathbf{K}}}{N^{\mathbf{K}}}\frac{\partial N^{\mathbf{K}}}{\partial\psi_{\mathbf{q}}^{\mathbf{K}*}} = 0. \tag{2.7}$$

For each crystal momentum $\mathbf{K}$, we solve Eqs. (2.6) and (2.7) by numerical means to obtain optimized $\lambda_{\mathbf{q}}^{\mathbf{K}}$ and $\psi_{\mathbf{q}}^{\mathbf{K}}$. The set of self-consistent equations resulting from Eqs. (2.6) and (2.7) is given in the Appendix.

Generalizations to include two or more particles in the variational calculation is straightforward. For the two-particle case, for example, one only needs to apply the projection operator[17]

$$\hat{P}^{\mathbf{K}} = \delta(\mathbf{K}-\hat{\mathbf{P}}) = N^{-1}\sum_{\mathbf{n}}\exp\left[i\mathbf{n}\cdot\left(\mathbf{K}-\sum_{\mathbf{k}}\mathbf{k}a_{\mathbf{k}}^{\dagger}a_{\mathbf{k}}-\sum_{\mathbf{q}}\mathbf{q}b_{\mathbf{q}}^{\dagger}b_{\mathbf{q}}\right)\right], \tag{2.8}$$

onto a localized wavefunction,

$$\sum_{\mathbf{nm}}\lambda_{\mathbf{nm}}a_{\mathbf{n}}^{\dagger}a_{\mathbf{m}}^{\dagger}\exp\left[-\sum_{\mathbf{l}}(\lambda_{\mathbf{nm,l}}b_{\mathbf{l}}^{\dagger}-\lambda_{\mathbf{nm,l}}^{*}b_{\mathbf{l}})\right]|0\rangle, \tag{2.9}$$

where $\hat{\mathbf{P}}$ is the crystal momentum of the system

$$\hat{\mathbf{P}} = \sum_{\mathbf{k}}\mathbf{k}a_{\mathbf{k}}^{\dagger}a_{\mathbf{k}} + \sum_{\mathbf{q}}\mathbf{q}b_{\mathbf{q}}^{\dagger}b_{\mathbf{q}}, \tag{2.10}$$

$\mathbf{n}$, $\mathbf{m}$, $\mathbf{l}$, and $\mathbf{j}$ are site indices for a finite lattice employed in the calculation here, and $\mathbf{q}$, $\mathbf{k}$, and $\mathbf{K}$ are momentum indices. The site–space particle (boson) operators $a_{\mathbf{n}}(b_{\mathbf{l}})$ are the Fourier transforms of $a_{\mathbf{k}}(b_{\mathbf{q}})$. The variational parameters $\lambda_{\mathbf{nm}}$ and $\lambda_{\mathbf{nm,l}}$ acquire an extra index $\mathbf{K}$ after the application of $\hat{P}^{\mathbf{K}}$. In fact, the single-particle Toyozawa ansatz Eq. (2.2) is obtained from a simple particle–boson structure,

$$|\Psi_L\rangle = \sum_{\mathbf{m}}\psi_{\mathbf{m}}a_{\mathbf{m}}^{\dagger}\exp\left[-\sum_{\mathbf{l}}(\lambda_{\mathbf{l}}b_{\mathbf{l}}^{\dagger}-\lambda_{\mathbf{l}}^{*}b_{\mathbf{l}})\right]|0\rangle, \tag{2.11}$$

via the projection operator $\hat{P}^{\mathbf{K}}$:

$$|\Phi^{\mathbf{K}}\rangle = \hat{P}^{\mathbf{K}}|\Psi_L\rangle. \tag{2.12}$$

Only the translationally-invariant components of the localized wave functions, Eqs. (2.9) and (2.11), with a total momentum $\mathbf{K}$ survive the application of $\hat{P}^{\mathbf{K}}$.

The ansatz wave function, Eq. (2.2) allows ample flexibility for the fermion and boson degrees of freedom to settle into a self-consistent state for each crystal momentum $\mathbf{K}$. In one-dimensional systems Eq. (2.2) was shown to provide some of the best wave functions for the Holstein Hamiltonian with diagonal and off-diagonal couplings.[17,21,22] Applications of Eq. (2.2) to two-dimensional fermion–boson systems, however, have remained elusive. In the remainder of the article we implement the above variational procedure to two practical problems.

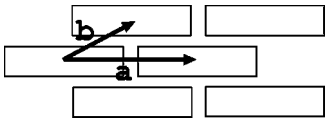

FIG. 1. The brick-work structure of PIC-Br *J*-aggregates. The lattice is elongated along the horizontal **a** direction.

III. SUPERRADIANCE IN *J*-AGGREGATES

Molecular dye aggregates have many technological applications such as sensitizers for silver halide materials in photographic films. Optical properties of dye aggregates differ from those of monomers due to intermolecular couplings which depend on relative positioning of molecular transition dipoles. For example, *J*-aggregates exhibit a characteristic sharp absorption peak (the *J*-band) below the monomer transition energy. The *J*-band corresponds to the delocalized excitons created by dipole interactions. The fluorescence band of *J*-aggregates is found to be the mirror image of the *J*-band with respect to the monomer absorption peak.[23] Therefore the absorption model of *J*-aggregates can be applied to emission as well. Superradiance (coherent spontaneous emission) is the enhanced radiative decay compared to that of a monomer as a result of the coherent nature of the electronic excited states.

It was argued that the superradiance of PIC-Br *J*-aggregates have to be modeled as a two-dimensional aggregate on a brick-work lattice.[6] An illustration of the lattice structure is shown in Fig. 1, where the horizontal axis in the brick-work lattice is labeled as **a**, and the other axis as **b**. We adopt the Einstein phonons and diagonal exiton–phonon coupling to describe the *J*-aggregates,

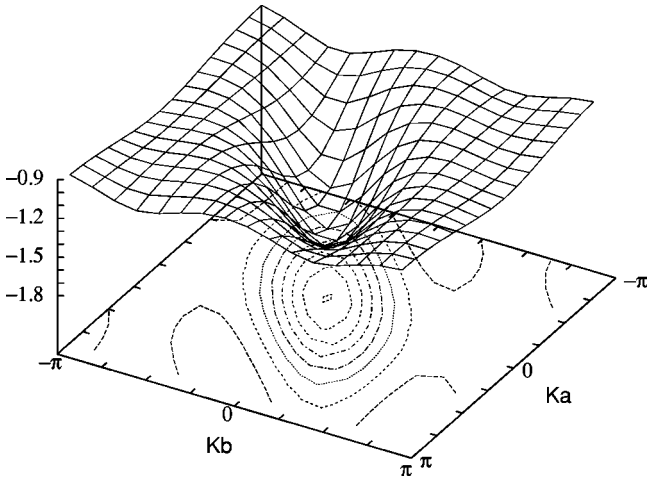

FIG. 2. Polaron band $E_{\mathbf{K}=(K_a,K_b)}$ (in units of ω) in the full Brillouin zone. $J_2=J_3=J_4=0.3\omega$, $J_1=0.1J_2$, and $g=1$.

$$\hat{H}_1=\sum_{\mathbf{k}} J_{\mathbf{k}} a_{\mathbf{k}}^{\dagger} a_{\mathbf{k}}+\omega\sum_{\mathbf{q}} b_{\mathbf{q}}^{\dagger} b_{\mathbf{q}} + \frac{g}{\sqrt{N}}\sum_{\mathbf{kq}} a_{\mathbf{k}-\mathbf{q}}^{\dagger} a_{\mathbf{k}}(b_{\mathbf{q}}^{\dagger}+b_{-\mathbf{q}}), \tag{3.1}$$

where the bare exciton band $J_{\mathbf{k}}$ has the form

$$J_{\mathbf{k}}=-J_1\cos(k_a)-J_2\cos(k_b)-J_3\cos(k_b-k_a) -J_4\cos(2k_b-k_a), \tag{3.2}$$

with k_a and k_b being components of $\mathbf{k}$ along $\mathbf{a}$ and $\mathbf{b}$ directions, respectively. Interactions from three pairs of nearest-neighbors (the J_1, J_2 and J_3 terms) and one pair of next-nearest-neighbors (the J_4 term) are included in Eq. (3.2). The electronic coupling parameters J_i $(i=1,...,4)$ are determined from the interactions of transition dipoles. J_1 is much smaller than other J's because of elongation of the brick lattice along $\mathbf{a}$ direction.

There may be phonon modes with nonuniform dispersions which are coupled diagonally or off-diagnonally to the electronic excitations in PIC-Br J-aggregates. Our model with Einstein phonons and diagonal exciton–phonon coupling is rather simplified in this respect. There are little experimental data on relevant phonon modes to constraint theory except the fact that coupling to low-energy acoustic phonons is unimportant because of the constant radiative lifetime up to 30 K. Exciton–acoustic-phonon coupling is therefore ruled out. In a previous publication on superradiance of light-harvesting antenna systems (LH2),[1] it was demonstrated that temperature dependence of superradiance is insensitive to the detailed forms of exciton–phonon coupling. Diagonal and off-diagonal couplings were found to generate similar superradiance-vs.-temperature plots. These are the rationale behind which we adopt Einstein phonons coupled diagonal to excitons in the first step of modeling the J-aggregates. Generalizations to nonuniform phonon dispersions off-diagonally coupled to excitons can be readily done within the framework of the Toyozawa ansatz.

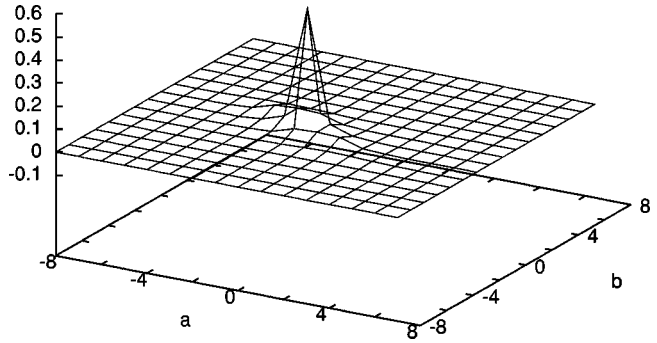

FIG. 3. Ground-state phonon displacements $\lambda_{\mathbf{n}=(a,b)}^{\mathbf{K}=(0,0)}$ for $J_2=J_3=J_4=0.3\omega$, $J_1=0.1J_2$, and $g=1$.

After optimization is carried out for $\lambda_{\mathbf{q}}^{\mathbf{K}}$ and $\psi_{\mathbf{q}}^{\mathbf{K}}$, and the polaron band $E_{\mathbf{K}}$ determined, the full density matrix at low temperatures (T small compared with ω) can be calculated from

$$\rho=Z^{-1}\sum_{\mathbf{K}} N_{\mathbf{K}}^{-1}|\Phi^{\mathbf{K}}\rangle e^{-E_{\mathbf{K}}/T}\langle\Phi^{\mathbf{K}}|, \tag{3.3}$$

where the partition function $Z\equiv\Sigma_{\mathbf{K}}\exp(-E_{\mathbf{K}}/T)$. The one-exciton reduced density matrix $\rho_{\mathbf{nm}}$ is defined as

$$\rho_{\mathbf{mn}}\equiv\mathrm{Tr}(\rho a_{\mathbf{m}}^{\dagger} a_{\mathbf{n}}). \tag{3.4}$$

The superradiance is calculated from[5,24]

$$L_s\equiv\sum_{\mathbf{mn}} \mathbf{d}_{\mathbf{m}}\cdot\mathbf{d}_{\mathbf{n}}\rho_{\mathbf{mn}}, \tag{3.5}$$

where $\mathbf{d}_{\mathbf{m}}$ is a unit vector pointing along the direction of the transition diople at site $\mathbf{m}$. If all transition dipoles are parallel, and translational invariance is taken into account ($\rho_{\mathbf{mn}}=\rho_{\mathbf{m-n}}$), then

$$L_s^{\parallel}=\sum_{\mathbf{mn}} \rho_{\mathbf{mn}}=N\sum_{\mathbf{l}=\mathbf{m}-\mathbf{n}} \rho_{\mathbf{l}}, \tag{3.6}$$

where N is the total number of chromophores.

Figure 2 shows the polaron band structure in the full Brillouin zone for electronic couplings $J_2=J_3=J_4=0.3\omega$, $J_1=0.1J_2$, and exciton–phonon coupling $g=1$. The flat topping of the band signifies the bottom of the one-phonon continuum where the polaron momenta is carried by its phonon

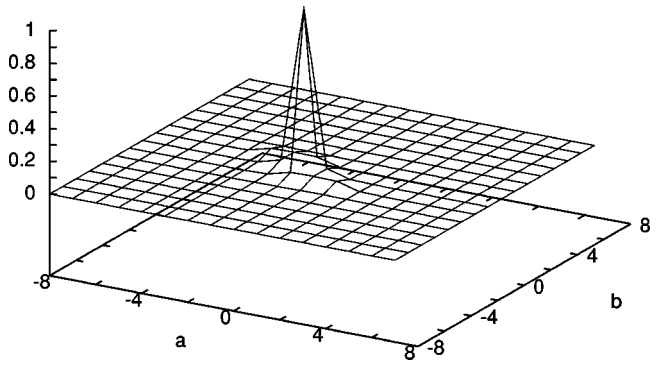

FIG. 4. Ground-state exciton amplitudes $\psi_{\mathbf{n}=(a,b)}^{\mathbf{K}=(0,0)}$ for $J_2=J_3=J_4=0.3\omega$, $J_1=0.1J_2$, and $g=1$. $\psi_{\mathbf{n}=(a,b)}^{\mathbf{K}=(0,0)}$ is normalized so that $\psi_{\mathbf{n}=(0,0)}^{\mathbf{K}=(0,0)}=1$.

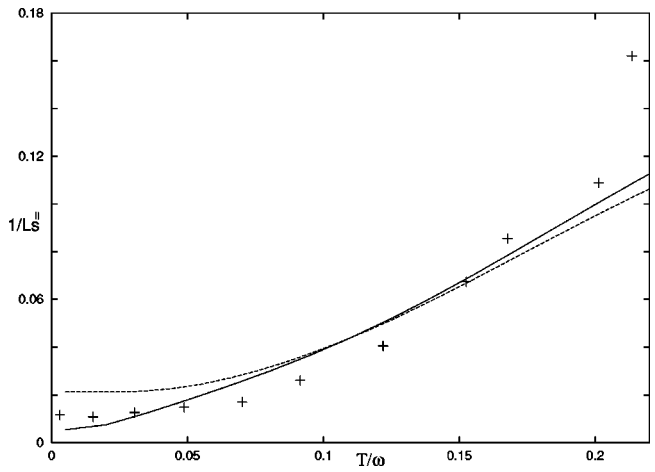

FIG. 5. Inversed superradiance $1/L_s^{\|}$ (radiative lifetime of an aggregate in units of the monomer lifetime) vs temperature. $J_2=J_3=J_4=0.3\omega$, $J_1=0.1J_2$, and $g=1$. Solid: 16×16 lattice. Dashed: 8×8 lattice. Points: experiment (Ref. 6).

cloud in significant portion.[24] The minimum of the band is located $\mathbf{K}=(0,0)$ where the exciton is more mobile along the $\mathbf{a}-2\mathbf{b}$ direction (the vertical direction in Fig. 1) than along the $\mathbf{a}$ or $\mathbf{a}+\mathbf{b}$ directions. Figures 3 and 4 display the variational parameters $\lambda_{\mathbf{q}}^{\mathbf{K}}$ and $\psi_{\mathbf{q}}^{\mathbf{K}}$ at $\mathbf{K}=(0,0)$, respectively. A spreading of both the phonon displacements and the exciton amplitudes over 3–4 sites is observed. In line with the band structure, the spread is also more pronounced along the $\mathbf{a}-2\mathbf{b}$ direction.

In Fig. 5 the radiative lifetime of the aggregate in units of the monomer lifetime (the inverse of superradiance) is plotted as a function of the temperature. The phonon frequency is assumed to be 656 K, and the monomer lifetime to 5555 ps. The solid curve is from a 16 by 16 lattice, and the dashed from an 8 by 8 lattice. The parameters are chosen to be the same as in Fig. 2. Agreements with the experimental data from Ref. 6 are reasonably good except for one highest temperature point. The discrepancy may be due to the fact that the aggregates are three-dimensional entities.

IV. HOLE MOTION IN AN ANTIFERROMAGNET

Interest in the problem of a single hole in a two-dimensional antiferromagnet is stimulated recently by photoemision measurements in the insulating cuprate $Sr_2CuO_2Cl_2$ (Refs. 25–29) and $Ca_2CuO_2Cl_2$ (Ref. 30) which allow a close comparison of the quasiparticle dispersion relation between theories[31–46] and experiments. In this section we apply the Toyozawa ansatz to calculate the quasiparticle dispersion for an itinerant hole in a two-dimensional antiferromagnet. We start from the linear spin–wave approximation of the $S=\frac{1}{2}$ antiferromagnetic background following Schmitt–Rink *et al.* and Kane *et al.* However, instead of resorting to perturbative expansions which often carry uncontrolled approximations, we employ a trial wave function of magnon coherent states to variationally compute the energy–momentum relation. Apart from its simplicity and reliability as compared with other methods, the approach clearly establishes the anticipated link[10–15,47] between the lattice polaron and the magnon-dressed hole by treating the two on an equal footing.

The Holstein–Primakoff spin–wave approximation may be derived from a $1/S$ expansion of the pure (updoped) Heisenberg Hamiltonian expressed in terms of Schwinger bosons.[32] The mean-field solution corresponds to a Nèel state with spins on one sublattice pointing down and spins on the other sublattice pointing up. The lowest-order fluctuations around the Nèel order in powers of the spin-deviation operators are described by the linear spin–wave approximation. Higher-order nonlinear spin–wave corrections have been shown to be small.[37] A thorough numerical demonstration of the accuracy of the spin–wave approximation was carried out by one of the authors in Ref. 48. In the linear spin-wave approximation,[31,32] only terms lowest in the spin-deviation operators are retained, and the spin Hamiltonian is diagonalized by a Bogoliubov transformation. The effective Hamiltonian reads

$$\hat{H}_2=\sum_{\mathbf{q}}\ \omega_{\mathbf{q}}b_{\mathbf{q}}^{\dagger}b_{\mathbf{q}}+\frac{tz}{\sqrt{N}}\sum_{\mathbf{kq}}\ h_{\mathbf{k}-\mathbf{q}}^{\dagger}h_{\mathbf{k}}[(u_{\mathbf{q}}\gamma_{\mathbf{k}-\mathbf{q}}+v_{\mathbf{q}}\gamma_{\mathbf{k}})b_{\mathbf{q}}^{\dagger}+(u_{\mathbf{q}}\gamma_{\mathbf{k}}+v_{\mathbf{q}}\gamma_{\mathbf{k}-\mathbf{q}})b_{-\mathbf{q}}], \tag{4.1}$$

where $h_{\mathbf{q}}(h_{\mathbf{q}}^{\dagger})$ and $b_{\mathbf{q}}(b_{\mathbf{q}}^{\dagger})$ are hole and magnon annihilation (creation) operators, respectively, z is the number of nearest-neighbors, N is the number of sites, and

$$\gamma_{\mathbf{q}}=\frac{1}{2}[\cos(q_x)+\cos(q_y)], \tag{4.2}$$

$$\omega_{\mathbf{q}}=JzS\sqrt{1-\alpha^2\gamma_{\mathbf{q}}^2}, \tag{4.3}$$

$$u_{\mathbf{q}}=\sqrt{\frac{JzS+\omega_{\mathbf{q}}}{2\omega_{\mathbf{q}}}}, \tag{4.4}$$

$$v_{\mathbf{q}}=-\mathrm{sgn}(\gamma_{\mathbf{q}})\sqrt{\frac{JzS-\omega_{\mathbf{q}}}{2\omega_{\mathbf{q}}}}. \tag{4.5}$$

J is the antiferromagnetic exchange energy between two spins on copper atoms, and $S=1/2$. We adopt the usual Bogoliubov coefficients $u_{\mathbf{q}}$ and $v_{\mathbf{q}}$. A square lattice with a lattice constant $a=1$ is assumed. Wave vectors of the reciprocal lattice are labeled by q_x and q_y. The magnon dispersion is denoted by $\omega_{\mathbf{q}}$. The parameter α is introduced to offer passage from the Ising limit ($\alpha=0$) to the Heisenberg limit ($\alpha=1$). The effective Hamiltonian, Eq. (4.1), bears close resemblance to the polaron Hamiltonian incorporating off-diagonal coupling.[21,22,49–52] Difficulties of treating off-diagonal coupling lie in finding reliable methods to diagonalize the Hamiltonian, Eq. (2.1).[49] As a consequence, off-diagonal coupling was customarily omitted.[52] In a recent work by Zhao *et al.*[22] the Toyozawa ansatz was utilized to solve the one-dimensional problem of simultaneous diagonal and off-diagonal exciton–phonon coupling. Results from the variational treatment are in excellent agreement with those from a mean-field theory with optimization[21] and a dynamical coherent potential approach.[53] This encourages applications of the Toyozawa wave function to other Hamiltonians. Calculations are carried out for 8 by 8 lattices. Due to sym-

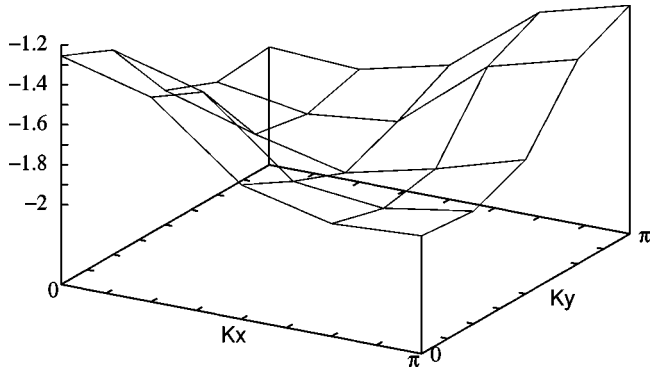

FIG. 6. Quasiparticle dispersion $E_{\mathbf{K}=(K_x,K_y)}$ (in units of t) in one-quarter of the Brillouin zone for the t-J model. $J/t=0.4$.

metry the computation needs only be performed for the irreducible part of the Brillouin zone which corresponds to one-sixteenth of the full zone area.

In Fig. 6 the quasiparticle dispersion of the Heisenberg spins is shown for $J/t=0.4$. The lowest energy state for the Heisenberg spins has a crystal momentum $(\pi/2,\pi/2)$. Around the points $(0,\pi)$ and $(\pi,0)$, a very flat band is observed. In agreement with previous theoretical results (see, e.g., Ref. 46), the effective mass along the direction from $(0,\pi)$ to $(\pi,0)$ is significantly larger than that along the direction from $(0,0)$ to (π,π). Width of the quasiparticle band is plotted against J/t in Fig. 7. A bandwidth maximum is reached around $J/t=0.9$.

V. DISCUSSION

We have proposed a general numerical method applicable to two-dimensional particle–boson systems with arbitrary forms of linear particle–boson interactions and boson dispersion relations. The Toyozawa ansatz is utilized for its relative efficiency, and for its flexibility to accommodate various forms of off-diagonal particle–boson couplings as compared to other methods (such as a recent density matrix approach to phonon Hilbert-space truncation).[54] Applications are made to model superradiance in PIC J-aggregates, and to study single-hole motion in a two-dimensional antiferromagnet.

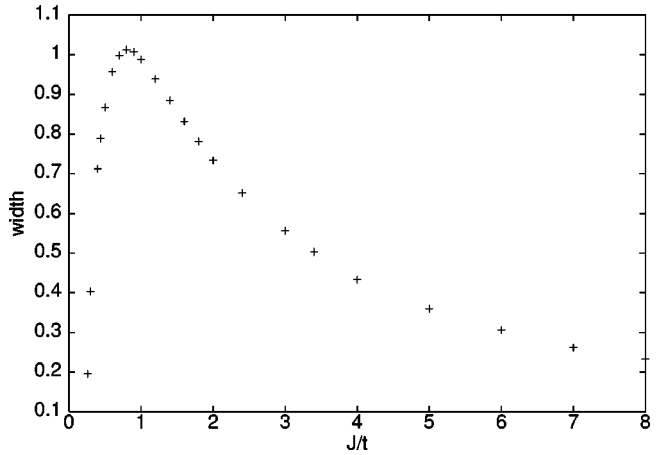

FIG. 7. Quasiparticle bandwidth (in units of t) plotted against J/t for the Heisenberg spins.

The dynamic-disorder model of superradiance has been previously developed and applied in a one-dimensional form to light-harvesting antenna complexes.[5,24] Phonon-induced localization is believed to be more relevant in PIC J-aggregates.[6] The brick-work lattice of PIC J-aggregates is entirely different from the ring-like structures of LH1 and LH2 for which one-dimensional models with periodic boundary conditions apply. The number of coherently emitting chromophores at low temperatures is significantly larger in PIC J-aggregates than in LH1 and LH2 as a result of the dimensionality. This has been clearly demonstrated by our model employing the generalized Holstein Hamiltonian. For example, a two-dimensional aggregate of size $16L_m$ (L_m is the size of a monomer) free of static inhomogeneities is needed in order for 256 monomers to emit coherently at low temperatures. In one dimension, however, this requires an aggregate size of $256L_m$ which can easily reach the upper size limit of superradiance—the size of the optical wavelength.

In Sec. IV we have reproduced many features of the dispersion relation of the t-J model variationally. The band structure as well as the band width as a function of J/t (cf. Figs. 6 and 7) are in agreement with previous theoretical results. The approach also serves as a direct link between the spin polaron and the traditional lattice polaron. Recent photoemission data[27] indicated a rather isotropic structure around the band minimum $(\pi/2,\pi/2)$ which was believed to result from direct oxygen–oxygen hopping t' on the same sublattice. The approach developed here still applies if t' is introduced into the model. Since the next-nearest hopping t' does not disturb the antiferromagnetic background, the t' term is therefore not coupled to the magnons. Its role is similar to that of the electronic transfer integral on the lattice polaron. Analytical tools such as the self-consistent Born approximation, which were quite successful in treating the t-J model, remain to be justified when applied to t-t'-J.[37,40] Our variational approach provides a reliable alternative to circumvent those speculative approximations discarding unexamined vertex corrections. In addition, as formulated in Sec. II, our approach can also be applied to the problem of two holes in an antiferromagnet which has recently attracted attention.[13,55]

ACKNOWLEDGMENTS

One of the authors (Y.Z.) would like to thank R. Hlubina and H. Q. Lin for discussions.

APPENDIX: THE SELF-CONSISTENT EQUATIONS FOR THE VARIATIONAL PARAMETERS

In this appendix we work out the self-consistent equations for $\lambda_{\mathbf{q}}^{\mathbf{K}}$ and $\psi_{\mathbf{q}}^{\mathbf{K}}$ in the variational procedure. The Hamiltonian, Eq. (2.1) has three terms:

$$\hat{H}=\hat{H}^a+\hat{H}^b+\hat{H}^{a-b}, \tag{A1}$$

which are the particle term, the boson term, and the particle–boson coupling term, respectively,

$$\hat{H}^a=\sum_{\mathbf{k}} J_{\mathbf{k}} a_{\mathbf{k}}^{\dagger} a_{\mathbf{k}}, \tag{A2}$$

$$\hat{H}^b=\sum_{\mathbf{q}} \omega_{\mathbf{q}} b_{\mathbf{q}}^{\dagger} b_{\mathbf{q}}, \tag{A3}$$

$$\hat{H}^{a-b}=\frac{1}{\sqrt{N}}\sum_{\mathbf{kq}} (M_{\mathbf{k},\mathbf{q}} a_{\mathbf{k}-\mathbf{q}}^{\dagger} a_{\mathbf{k}} b_{\mathbf{q}}^{\dagger}+\text{H.c.}). \tag{A4}$$

The expectation values of each term in the trial state are given below:

$$\langle \Phi^{\mathbf{K}}|\hat{H}^a|\Phi^{\mathbf{K}}\rangle = N^{-1}\sum_{\mathbf{k}} S^{\mathbf{K}}_{\mathbf{K}-\mathbf{k}} J_{\mathbf{k}} |\psi^{\mathbf{K}}_{\mathbf{k}}|^2, \tag{A5}$$

$$\langle \Phi^{\mathbf{K}}|\hat{H}^b|\Phi^{\mathbf{K}}\rangle = N^{-2}\sum_{\mathbf{kq}} \omega_{\mathbf{q}} S^{\mathbf{K}}_{\mathbf{K}-\mathbf{k}-\mathbf{q}} |\psi^{\mathbf{K}}_{\mathbf{k}}|^2 |\lambda^{\mathbf{K}}_{\mathbf{q}}|^2, \tag{A6}$$

$$\langle \Phi^{\mathbf{K}}|\hat{H}^{a-b}|\Phi^{\mathbf{K}}\rangle = -N^{-2}\sum_{\mathbf{kq}} \psi^{\mathbf{K}*}_{\mathbf{k}} \psi^{\mathbf{K}}_{\mathbf{k}+\mathbf{q}} (M_{\mathbf{k}+\mathbf{q},\mathbf{q}} S^{\mathbf{K}}_{\mathbf{K}-\mathbf{k}-\mathbf{q}} \lambda^{\mathbf{K}*}_{\mathbf{q}} + M^{*}_{\mathbf{k},-\mathbf{q}} S^{\mathbf{K}*}_{\mathbf{K}-\mathbf{k}} \lambda^{\mathbf{K}}_{-\mathbf{q}}). \tag{A7}$$

Here, $S^{\mathbf{K}}_{\mathbf{k}}$ is the Fourier transform of the generalized Debye–Waller factors $S^{\mathbf{K}}_{\mathbf{n}}$,

$$S^{\mathbf{K}}_{\mathbf{k}}=\sum_{\mathbf{n}} e^{-i\mathbf{k}\cdot\mathbf{n}} S^{\mathbf{K}}_{\mathbf{n}}, \tag{A8}$$

$$S^{\mathbf{K}}_{n}=\exp\left[N^{-1}\sum_{\mathbf{q}} |\lambda^{\mathbf{K}}_{\mathbf{q}}|^2 (e^{i\mathbf{q}\cdot\mathbf{n}}-1)\right]. \tag{A9}$$

The trial state is in general not normalized,

$$N^{\mathbf{K}}=\langle \Phi^{\mathbf{K}}|\Phi^{\mathbf{K}}\rangle = N^{-1}\sum_{\mathbf{k}} S^{\mathbf{K}}_{\mathbf{K}-\mathbf{k}} |\psi^{\mathbf{K}}_{\mathbf{k}}|^2. \tag{A10}$$

We define the total energy as

$$E_{\mathbf{K}}=\frac{H^{\mathbf{K}}}{N^{\mathbf{K}}}. \tag{A11}$$

Minimization of $E_{\mathbf{K}}$ with respect to the boson displacements $\lambda^{\mathbf{K}*}_{\mathbf{q}}$ leads to

$$\lambda^{\mathbf{K}}_{\mathbf{q}}=\frac{L^{\mathbf{K}}_{\mathbf{q}}}{\omega_{\mathbf{q}} N^{\mathbf{K}}_{\mathbf{q}}+H^{\mathbf{K}}_{\mathbf{q}}-N^{\mathbf{K}}_{\mathbf{q}} E_{\mathbf{K}}}, \tag{A12}$$

where

$$L^{\mathbf{K}}_{\mathbf{q}}=N^{-1}\sum_{\mathbf{k}} M_{\mathbf{k}+\mathbf{q},\mathbf{q}} S^{\mathbf{K}}_{\mathbf{K}-\mathbf{k}-\mathbf{q}} \psi^{\mathbf{K}*}_{\mathbf{k}} \psi^{\mathbf{K}}_{\mathbf{k}+\mathbf{q}}, \tag{A13}$$

$$N^{\mathbf{K}}_{\mathbf{q}}=N^{-1}\sum_{\mathbf{k}} S^{\mathbf{K}}_{\mathbf{K}-\mathbf{k}-\mathbf{q}} |\psi^{\mathbf{K}}_{\mathbf{k}}|^2, \tag{A14}$$

and $H^{\mathbf{K}}_{\mathbf{q}}$ is the sum of three terms:

$$H^{\mathbf{K}}_{\mathbf{q}}=H^{a}_{\mathbf{q}}+H^{b}_{\mathbf{q}}+H^{a-b}_{\mathbf{q}}, \tag{A15}$$

$$H^{a}_{\mathbf{q}}=N^{-1}\sum_{\mathbf{k}} S^{\mathbf{K}}_{\mathbf{K}-\mathbf{k}-\mathbf{q}} J_{\mathbf{k}} |\psi^{\mathbf{K}}_{\mathbf{k}}|^2, \tag{A16}$$

$$H^{b}_{\mathbf{q}}=N^{-2}\sum_{\mathbf{kq}'} \omega_{\mathbf{q}'} S^{\mathbf{K}}_{\mathbf{K}-\mathbf{k}-\mathbf{q}-\mathbf{q}'} |\psi^{\mathbf{K}}_{\mathbf{k}}|^2 |\lambda^{\mathbf{K}}_{\mathbf{q}'}|^2, \tag{A17}$$

$$H^{a-b}_{\mathbf{q}}=-N^{-2}\sum_{\mathbf{kq}'} \psi^{\mathbf{K}*}_{\mathbf{k}} \psi^{\mathbf{K}}_{\mathbf{k}+\mathbf{q}'} (M_{\mathbf{k}+\mathbf{q}',\mathbf{q}'} S^{\mathbf{K}}_{\mathbf{K}-\mathbf{k}-\mathbf{q}-\mathbf{q}'} \lambda^{\mathbf{K}*}_{\mathbf{q}'} + M^{*}_{\mathbf{k},-\mathbf{q}'} S^{\mathbf{K}*}_{\mathbf{K}-\mathbf{k}-\mathbf{q}} \lambda^{\mathbf{K}}_{-\mathbf{q}'}). \tag{A18}$$

Turning to minimization of $E_{\mathbf{K}}$ with respect to $\psi^{\mathbf{K}*}_{\mathbf{k}}$, one arrives at

$$\psi^{\mathbf{K}}_{\mathbf{k}}=\frac{U^{\mathbf{K}}_{\mathbf{k}}}{V^{\mathbf{K}}_{\mathbf{k}}-(E_{\mathbf{K}}-J_{\mathbf{k}}) S^{\mathbf{K}}_{\mathbf{K}-\mathbf{k}}}, \tag{A19}$$

where

$$U^{\mathbf{K}}_{\mathbf{k}}=N^{-1}\sum_{\mathbf{q}} \psi^{\mathbf{K}}_{\mathbf{k}+\mathbf{q}} (M_{\mathbf{k}+\mathbf{q},\mathbf{q}} S^{\mathbf{K}}_{\mathbf{K}-\mathbf{k}-\mathbf{q}} \lambda^{\mathbf{K}*}_{\mathbf{q}} + M^{*}_{\mathbf{k},-\mathbf{q}} S^{\mathbf{K}*}_{\mathbf{K}-\mathbf{k}} \lambda^{\mathbf{K}}_{-\mathbf{q}}) \tag{A20}$$

and

$$V^{\mathbf{K}}_{\mathbf{k}}=N^{-1}\sum_{\mathbf{q}} \omega_{\mathbf{q}} S^{\mathbf{K}}_{\mathbf{K}-\mathbf{k}-\mathbf{q}} |\lambda^{\mathbf{K}}_{\mathbf{q}}|^2. \tag{A21}$$

[1] D. Emin and M. S. Hillery, Phys. Rev. B **39**, 6575 (1989).
[2] X. F. Wang and X. L. Lei, Solid State Commun. **91**, 513 (1994); H. Y. Zhou and S. W. Gu, *ibid.* **91**, 725 (1994).
[3] Q. Niu, P. Ao, and D. J. Thouless, Phys. Rev. Lett. **72**, 1706 (1994).
[4] F. C. Spano, J. R. Kuklinski, and S. Mukamel, Phys. Rev. Lett. **65**, 211 (1990).
[5] T. Meier, Y. Zhao, V. Chernyak, and S. Mukamel, J. Chem. Phys. **107**, 3876 (1997).
[6] E. O. Potma and D. A. Wiersma, J. Chem. Phys. **108**, 4894 (1998).
[7] J. Ray and N. Makri, J. Phys. Chem. A **103**, 9417 (1999).
[8] V. Novoderezhkin, R. Monshouwer, and R. van Grondelle, J. Phys. Chem. B **103**, 10540 (1999); Biophys. J. **77**, 666 (1999).
[9] T. Polivka, T. Pullerits, J. L. Herek, and V. Sundström, J. Phys. Chem. B **104**, 1088 (2000).
[10] L. Yu, Z. B. Su, and Y. M. Li, Chin. J. Phys. (Taipei) **31**, 579 (1993).
[11] Y. M. Li, N. d'Ambrumenil, L. Yu, and Z. B. Su, Phys. Rev. B **53**, 14717 (1996).
[12] H. Barentzen, Phys. Rev. B **53**, 5598 (1996).
[13] V. I. Belinicher, A. L. Chernyshev, and V. A. Shubin, Phys. Rev. B **56**, 3381 (1997); A. L. Chernyshev, P. W. Leung, and R. J. Gooding, *ibid.* **58**, 13594 (1998).
[14] M.-F. Yang, Phys. Rev. B **55**, 56 (1997).
[15] T. Li and Z. Z. Gan, J. Phys.: Condens. Matter **10**, 8007 (1998).
[16] Y. Toyozawa, Prog. Theor. Phys. **26**, 29 (1961).
[17] Y. Zhao, D. W. Brown, and K. Lindenberg, J. Chem. Phys. **107**, 3159 (1997); **107**, 3179 (1997); **106**, 5622 (1997); A. Romero, D. W. Brown, and K. Lindenberg, *ibid.* **109**, 6540 (1998).
[18] V. M. Buinmistrov and S. I. Pekar, Sov. Phys. JETP **5**, 970 (1957).
[19] E. Jeckelman and S. R. White, Phys. Rev. B **57**, 6376 (1998).
[20] J. Bonca, S. A. Trugman, and I. Batistić, Phys. Rev. B **60**, 1633 (1999).
[21] Y. Zhao, D. W. Brown, and K. Lindenberg, J. Chem. Phys. **100**, 2335 (1994).
[22] Y. Zhao, D. W. Brown, and K. Lindenberg, J. Chem. Phys. **106**, 2728 (1997).
[23] G. Scheibe, in *Optische Anregung Organischer Systeme* 2. Internationales Farbesymposium, edited by W. Foerst (Verlag Chemie, Weinheim, 1966).
[24] Y. Zhao, T. Meier, W. M. Zhang, V. Chernyak, and S. Mukamel, J. Phys. Chem. B **103**, 3954 (1999).
[25] Z.-X. Shen *et al.*, Science **267**, 343 (1995).
[26] D. S. Dessau *et al.*, Phys. Rev. Lett. **71**, 2781 (1993).
[27] B. O. Wells *et al.*, Phys. Rev. Lett. **74**, 964 (1995); S. LaRosa *et al.*, Phys. Rev. B **56**, R525 (1997).
[28] K. Gofron *et al.*, Phys. Rev. Lett. **73**, 3302 (1994).
[29] C. Kim *et al.*, Phys. Rev. Lett. **74**, 4245 (1998).
[30] F. Ronning *et al.*, Science **282**, 2067 (1998).

[31] S. Schmitt-Rink, C. M. Varma, and A. E. Ruckenstein, Phys. Rev. Lett. **60**, 2793 (1988).
[32] C. L. Kane, P. A. Lee, and N. Read, Phys. Rev. B **39**, 6880 (1989).
[33] Z. B. Su, Y. M. Li, W. Y. Lai, and L. Yu, Phys. Rev. Lett. **63**, 1318 (1989).
[34] A. V. Sherman, Solid State Commun. **76**, 321 (1990); Physica C **171**, 395 (1990).
[35] G. Martinez and P. Horsh, Phys. Rev. B **44**, 317 (1991).
[36] F. Marsiglio *et al.*, Phys. Rev. B **43**, 10882 (1991).
[37] Z. Liu and E. Manousakis, Phys. Rev. B **51**, 3156 (1995); **45**, 2425 (1992).
[38] A. Nazarenko *et al.*, Phys. Rev. B **51**, 8676 (1995).
[39] T. K. Lee and C. T. Shih, Phys. Rev. B **55**, 5983 (1997).
[40] K. J. E. Vos and R. J. Gooding, Z. Phys. B: Condens. Matter **101**, 79 (1996).
[41] P. W. Leung and R. J. Gooding, Phys. Rev. B **52**, 15711 (1995).
[42] B. Kyung and R. A. Ferrell, Phys. Rev. B **54**, 10125 (1996).
[43] A. Ramsak, and P. Horsh, Phys. Rev. B **48**, 10559 (1995).
[44] A. L. Chernyshev and P. W. Leung, Phys. Rev. B **60**, 1592 (1999).
[45] T. Tohyama *et al.*, cond-mat/9904231.
[46] M. Brunner, F. F. Assaad, and A. Murammatsu, cond-mat/0002321.
[47] L. P. Gorkov (private communication).
[48] G. H. Chen, H.-Q. Ding, and W. A. Goddard III, Phys. Rev. B **46**, 2933 (1992).
[49] R. W. Munn and R. Silbey, J. Chem. Phys. **83**, 1843 (1994).
[50] K. S. Song, J. Phys. Soc. Jpn. **26**, 1131 (1969).
[51] M. Umehara, J. Phys. Soc. Jpn. **47**, 852 (1979).
[52] G. D. Mahan *Many-Particle Physics* (Plenum, New York, 1981).
[53] T. Kato, F. Sasaki, and S. Kobayashi, Chem. Phys. Lett. **303**, 649 (1999).
[54] C. L. Zhang, E. Jeckelmann, and S. R. White, Phys. Rev. B **60**, 14092 (1999); Phys. Rev. Lett. **80**, 2661 (1998).
[55] H. Barentzen and V. Oudovenko, Europhys. Lett. **47**, 227 (1999).